Clim. Past Discuss., https://doi.org/10.5194/cp-2018-152
Manuscript under review for journal Clim. Past
Discussion started: 7 November 2018

Climate of the Past Discussions

Insensitivity of alkenone carbon isotopes to atmospheric CO_2 at low to moderate CO_2 levels

Marcus P.S. Badger*[1,2], Thomas B. Chalk[3,4], Gavin L. Foster[3], Paul R. Bown[5], Samantha J. Gibbs[3], Philip F. Sexton[1], Daniela N. Schmidt[6,7], Heiko Pälike[8], Andreas Mackensen[9] and Richard D. Pancost[2,7]

[1]School of Environment, Earth & Ecosystem Sciences, The Open University, Milton Keynes, MK7 6AA, UK
[2]Organic Geochemistry Unit, School of Chemistry, School of Earth Sciences, University of Bristol, Bristol, BS8 1TS, UK
[3]School of Ocean and Earth Science, National Oceanography Centre Southampton, University of Southampton, Southampton SO14 3ZH, UK
[4]Department of Physical Oceanography, Woods Hole Oceanographic Institution, Woods Hole, MA, 02543, USA
[5]Department of Earth Sciences, University College London, London, WC1E 6BT, UK
[6]School of Earth Sciences, University of Bristol, Wills Memorial Building, Queens Road, Bristol, BS8 1RJ, UK
[7]The Cabot Institute, University of Bristol, Bristol BS8 1UJ, UK
[8]MARUM – Center for Marine Environmental Sciences, University of Bremen, Bremen, Germany
[9]Alfred Wegener Institute for Polar and Marine Research, Am Alten Hafen 26, 27568 Bremerhaven, Germany

Correspondence to: Marcus P.S. Badger (marcus.badger@open.ac.uk)

Abstract Atmospheric pCO_2 is a critical component of the global carbon system and is considered to be the major control of Earth's past, present and future climate. Accurate and precise reconstructions of its concentration through geological time are, therefore, crucial to our understanding of the Earth system. Ice core records document pCO_2 for the past 800 kyrs, but at no point during this interval were CO_2 levels higher than today. Interpretation of older pCO_2 has been hampered by discrepancies during some time intervals between two of the main ocean-based proxy methods used to reconstruct pCO_2: the carbon isotope fractionation that occurs during photosynthesis as recorded by haptophyte biomarkers (alkenones) and the boron isotope composition ($\delta^{11}B$) of foraminifer shells. Here we present alkenone and $\delta^{11}B$-based pCO_2 reconstructions generated from the same samples from the Plio-Pleistocene at ODP Site 999 across a glacial-interglacial cycle. We find a muted response to pCO_2 in the alkenone record compared to contemporaneous ice core and $\delta^{11}B$ records, suggesting caution in the interpretation of alkenone-based records at low pCO_2 levels. This is possibly caused by the physiology of CO_2 uptake in the haptophytes. Our new understanding resolves some of the inconsistencies between the proxies and highlights that caution may be required when interpreting alkenone-based reconstructions of pCO_2.

Clim. Past Discuss., https://doi.org/10.5194/cp-2018-152
Manuscript under review for journal Clim. Past
Discussion started: 7 November 2018

Climate of the Past Discussions

1. **Introduction**

Understanding the absolute level and evolution of atmospheric pCO_2 through geological time is essential to our understanding of the Earth's Climate System. As both a fundamental, first order control, and a contributor to multiple dynamic feedbacks, atmospheric pCO_2 is critical in setting Earth's surface temperature (Lacis et al., 2010). Reconstructing pCO_2 evolution improves the understanding of both the mechanisms behind past climate change (Chalk et al., 2017) , and provides novel constraints on climate sensitivities (Martínez-Botí et al., 2015b; PALAEOSENS, 2012). This then allows ground-truthing of our understanding the climate and the Earth system models that are used for predicting future climate change.

Over the past two decades, two common marine-based CO_2 proxies have emerged – alkenone-based ε_p values ($CO_{2(\varepsilon p\text{-}alk)}$), utilising the carbon isotopic fractionation imparted during photosynthesis in a subgroup of haptophytes (Bidigare et al., 1997), and planktic foraminiferal $\delta^{11}B$ values ($CO_{2(\delta 11Bplank)}$), based on the pH control of boron speciation and isotopic fractionation in seawater (Hemming and Hanson, 1992). Multiple records of atmospheric pCO_2 now exist for the Cenozoic from both methods, showing a broadly similar long-term trend from a high-CO_2 greenhouse world of the early Cenozoic to a low-CO_2 bi-polar glaciated world of the present (Anagnostou et al., 2016; Pagani et al., 2005, 2011; Pearson et al., 2009; Sosdian et al., 2018; Super et al., 2018).

However, discrepancies have recently become apparent between both methods when applied to the last 20 Ma (Badger et al., 2013b, 2013a). Specifically, the $CO_{2(\varepsilon p\text{-}alk)}$ reconstructions often suggest a lower magnitude of short-term pCO_2 change compared to that from $CO_{2(\delta 11Bplank)}$ (Badger et al., 2013b). Whilst this could be partially explained by mismatches between the sampling intervals, or by the influence of local surface water disequilibrium with the atmosphere with respect to CO_2, this discrepancy remains even for records generated from exactly the same sediment samples (Badger et al., 2013b vs Martínez-Botí et al., 2015). Both the $CO_{2(\varepsilon p\text{-}alk)}$ and $CO_{2(\delta 11Bplank)}$ have been used to estimate Earth system sensitivity in the Pliocene (e.g. Pagani et al., (2009) vs. Martínez-Botí et al., (2015)) with differing results; although this is at least partly due to the different approaches used to calculate Earth system sensitivity in the two studies, it is also due to the differences in reconstructed pCO_2 from the two approaches.

Clim. Past Discuss., https://doi.org/10.5194/cp-2018-152
Manuscript under review for journal Clim. Past
Discussion started: 7 November 2018

The $CO_{2(\varepsilon p\text{-}alk)}$ and $CO_{2(\delta 11Bplank)}$ palaeobarometers are both based on mechanistic frameworks that have been calibrated in either the modern ocean or laboratory culture (Bidigare et al., 1997; Hemming and Hanson, 1992; Pagani et al., 2002; Sanyal and Hemming, 1996). These proxies can be further ground-truthed in the recent geological past, when ice core records provide high-quality pCO_2 data for the last 800 kyrs (Bereiter et al., 2015). In previous work, both $CO_{2(\delta 11Bplank)}$ (Chalk et al., 2017; Foster, 2008; Foster and Sexton, 2014; Henehan et al., 2013; Hönisch and Hemming, 2005; Sanyal et al., 1995) and $CO_{2(\varepsilon p\text{-}alk)}$ (Jasper and Hayes, 1990) yield pCO_2 records similar in absolute value and amplitude of change to those derived from ice cores. However, the emerging discrepancies between the two methods (Badger et al., 2013a, 2013b; Martínez-Botí et al., 2015a) necessitate revisiting this validation, both between the two proxies, and between marine proxy and ice core reconstructions.

The ice core records pCO_2 of the Pleistocene glacial-interglacial cycles (Bereiter et al., 2015; Petit et al., 1999) provide an opportunity for cross-calibrating proxy methods for determining atmospheric pCO_2 in the geological archive ($CO_{2(\varepsilon p\text{-}alk)}$ and $CO_{2(\delta 11Bplank)}$) with the direct-CO_2 measurements from the ice cores.

1.2 Study Site

Ocean Drilling Program Site 999 is located in the Caribbean Sea (12° 44.639’ N, 78° 44.360’ W, 2838m water depth; Figure 1), has an orbitally calibrated age model and has been used previously for CO_2 reconstructions. Our temporal sampling resolution is ~6 kyrs in the Pleistocene and ~9 kyrs in the Pliocene. Although $CO_{2(\varepsilon p\text{-}alk)}$ and $CO_{2(\delta 11Bplank)}$ are independent of one another in many respects, they both rely on assumptions about the equilibrium of surface seawater with the atmosphere with respect to CO_2, sea surface temperature, and on well-constrained age models, which can make direct comparison between records from different sites difficult. Here we overcome these problems by producing $CO_{2(\varepsilon p\text{-}alk)}$ and $CO_{2(\delta 11Bplank)}$ records from identical horizons in the same deep ocean sediment core in 1) the late Pleistocene, permitting direct comparison to ice core data (Figure 2a, Figure 3), and 2) across the intensification of Northern Hemisphere glaciation (INHG) in the Pliocene (Martínez-Botí et al., 2015b; Seki et al., 2010) (Figure 2b).

In terms of CO_2, ODP Site 999 in the Caribbean Sea is today slightly out of equilibrium with the atmosphere, with surface waters a little oversaturated in CO_2, providing a small net source of CO_2 to the atmosphere (~21 µatm; Takahashi et al., 2009). However the site has been shown to be suitable for recording past changes in pCO_2 (Foster, 2008; Foster and Sexton, 2014)

Clim. Past Discuss., https://doi.org/10.5194/cp-2018-152
Manuscript under review for journal Clim. Past
Discussion started: 7 November 2018

and the air-sea equilibrium is not thought to have changed significantly from the Pliocene to today (see discussion in Bartoli et al., 2011). It is one of few sites where both alkenone and boron isotope records can be acquired given the good preservation of both foraminifera and organic matter (Badger et al., 2013b; Foster, 2008; Foster and Sexton, 2014; Martínez-Botí et al., 2015b), and Pliocene records of both are available (Badger et al., 2013b; Bartoli et al., 2011; Martínez-Botí et al., 2015b). It also has been demonstrated previously to record glacial-interglacial cycles of pH/CO_2 (Foster, 2008; Henehan et al., 2013) and a Pleistocene $CO_{2(\delta 11Bplank)}$ record from 0-250 ka has been recently published (Chalk et al., 2017).

2 Methods

2.1 Alkenone isotopes

Our new alkenone based CO_2 record was calculated following Badger et al., (2013b), with modern day phosphate used in the estimation of the 'b' term, UK37' temperatures, and modern day salinity. Samples were freeze dried, ground to a fine powder by hand, and extracted by Soxhlet apparatus using a dichloromethane (DCM) / methanol azeotrope (2:1, *v/v*) refluxing for 24 hours. Total lipid extracts were divided into three fractions (F) by small (4 cm) silica chromatography columns, with fractions eluting in 3 mL of *n*-hexane (F1), DCM (F2) and ethyl acetate/*n*-hexane (1:3. *v:v*, F3) respectively. Alkenones eluted in F2. Alkenone isotope analyses were performed using a ThemoFisher Delta V connected via a Gas Chromatograph (GC) isolink and ConFlo IV to a Trace GC.

The alkenone isotope $\delta^{13}C$ value is used to calculate the total carbon isotope fractionation that occurs during algal growth (ε_p). This isotopic fractionation has been shown to be controlled by $[CO_2]_{(aq)}$ (equation 1; Jasper & Hayes 1990) which can then be converted to atmospheric CO_2 using Henry's law.

Equation 1. $$\varepsilon_p = \varepsilon_f - \frac{b}{[CO_2]_{(aq)}}$$

To calculate ε_p from alkenone $\delta^{13}C$ vales the carbon isotopic composition of DIC is required, this is calculated from planktic foraminiferal calcite $\delta^{13}C$, whilst the fractionation which occurs during carbon fixation (ε_f), is here assumed constant. The'b'

term is the sum of other physiological factors (such as growth rate and cell size) which is estimated from the relationship shown in the modern ocean between 'b' and dissolved reactive phosphate $[PO_4^{3-}]$. Further details of the treatment can is detailed in Badger et al., (2013b).

Error bars in relevant figures are all 1sd and based on a full Monte Carlo propagation (n=10000) of the following uncertainties: ±2 °C and ±0.1 ‰ were applied to temperature and foraminiferal calcite $\delta^{13}C$, (normal probability function (pdf), 2σ error) and ±2 and ±0.1 to salinity and $[PO_4^{3-}]$, respectively (2σ; uniform pdf). Uncertainties on alkenone $\delta^{13}C$ were estimated from replicate runs and calcite $\delta^{13}C$ from repeat runs of an internal standard. Integrated analytical and calibration uncertainties for alkenone based temperatures were estimated and conservative estimates of likely variation for salinity and $[PO_4^{3-}]$ were used. An 11 % error on the slope of $b=a[PO_4^{3-}]+c$ was assumed, where a = 116.96 and c = 81.41 (Pagani et al., 1999).

For consistency with the $CO_{2(\delta 11Bplank)}$ record for this Site, we now adjust for the disequilibrium, and thus, have recalculated the included values of Badger et al., (2013b) accordingly. SSTs for our new Pliocene data were published in Davis et al., (2013).

2.2 Boron Isotopes

Boron isotope data were published in (Chalk et al., 2017) and are from the same core samples as our alkenone measurements. *Globigerinoides ruber sensu stricto* (white, n ~ 200 individuals from 300-355µm) samples were measured for boron isotope composition on Thermo Scientific Neptune MC-ICPMS at the University of Southampton according to methods described elsewhere (Foster et al., 2013; Martínez-Botí et al., 2015b; Rae et al., 2011). Analytical uncertainty is given by the external reproducibility of repeat analyses of Japanese Geological Survey Porites coral standard (JCP) at the University of Southampton following Henehan et al., (2013) and is typically <0.2 ‰ (at 95 % confidence). Metal element:calcium ratios (Li, Mg, B, Na, Al, Mn, Ba, Sr, Cd, U, Nd, and Fe) were analyzed using an Thermo Element 2XR ICP-MS at the University of Southampton). Here, these data are used to assess adequacy of clay removal (Al/Ca <100 µmol/mol) and to generate down core temperature. pH and CO_2 were calculated using a Monte Carlo approach (uncertainties are 2sd, n = 10,000 replicates) using R (R Core Team, 2015), for pH we use a boron isotopic composition of seawater of 39.6 ‰ (2sd of 0.1, Foster et al. 2010) and experimentally determined isotopic fractionation factor (1.027, Klochko et al., 2006) as well as the species specific calibration

Clim. Past Discuss., https://doi.org/10.5194/cp-2018-152
Manuscript under review for journal Clim. Past
Discussion started: 7 November 2018

for *G. ruber* of Henehan et al 2013 (also with incorporated uncertainties). For the CO_2 calculations we use a range of salinity and total alkalinity (Talk) that encompasses the modern values (34-37 and 2100-2500 µM, respectively, both with a uniform rather than normal probability distribution. Temperature was determined using Mg/Ca of *G. ruber* following established methods (Delaney and Boyle, 1985; Evans and Müller, 2012)). Inorganic chemical constants were used from the seacarb package in R (Gattuso et al., 2015), and using published values for the pKB (Dickson, 1990). Values from Foster, (2008) were recalculated to match this approach. All uncertainties are included in our simulation and are roughly equivalent to those assumed for the alkenone data and are exactly the same as those used for Martinez-Boti et al. 2015 excluding the $\delta^{11}B_{sw}$, thus providing a fair comparison.

2.3 Coccolith length measurements

The uptake of CO_2 into the coccolithophore cell is effected by the cell size and geometry (Laws et al., 1997; Popp et al., 1998), using alkenones limits the variation of cell geometry by restricting the source organism to one with exclusively spherical cells, but some change in cell size is possible. . Coccolith size is used as an semi-quantitative proxy for cell size because coccolith size is typically larger on larger cells, with that relationship being broadly consistent within a single taxonomic group where growth behaviour is broadly comparable (Gibbs et al., 2013; Henderiks, 2008; Sheward et al., 2017). Long-axis coccolith length measurements were therefore taken from 100 specimens of the family Noelaerhabdaceae per sample from standard smear slides. Specimens were imaged at 1500x magnification and measured using CellD software.

2.4 Age Model

For the interval 0-500 ka, we generated a detailed age model by tuning the planktic foraminifer (*G. ruber*) $\delta^{18}O$ record from Site 999 (at ~0.5 to 2.0 kyr resolution) (Schmidt et al., 2006) to the LR04 benthic $\delta^{18}O$ stack (Lisiecki and Raymo, 2005) using the Analyseries software (Paillard et al., 1996), the Pliocene portion of Site 999 is part the LR04 stack and that astronomically tuned age model is used here (Lisiecki and Raymo, 2005).

2.5 Bayesian exploration of $CO_{2(\varepsilon p\text{-}alk)}$ input variables

In order to examine the influence of the various input parameters for the calculation of pCO_2 from alkenone $\delta^{13}C$ values, we carry out a second set of Monte Carlo simulations (n=100,000) with expanded uncertainty. In this case, we more fully explore

Clim. Past Discuss., https://doi.org/10.5194/cp-2018-152
Manuscript under review for journal Clim. Past
Discussion started: 7 November 2018

uncertainty space using the following input uncertainties (at 95 % confidence or full range): SST (normal distribution, ± 6 °C), ε_f (uniform distribution, 24 to 28), b (normal distribution, ± 40), CO_2 disequilibrium (20 ± 20). These input distributions are our *prior* distributions. We then evaluate the CO_2 output for each alkenone sample against synchronous ice core pCO_2 and boron isotope pCO_2 for the Pleistocene and Pliocene, respectively. By only selecting those simulated alkenone pCO_2 levels that agree with ice core or $pCO_{2(\delta 11Bplank)}$ (including associated uncertainties), we can re-evaluate the input distributions (our *posterior*) and gain insights into the relative importance of each of the input variables in potentially driving the observed disagreements in pCO_2. Uncertainties in the $pCO_{2(\delta 11Bplank)}$ are as described above, and we apply an uncertainty of ± 6 ppm (2s) for the ice core pCO_2 record (Ahn et al., 2012).

3 Results and Discussion

Alkenone and *G. ruber* $\delta^{13}C$ values (Figure 3a,e) were used to calculate ε_p values (Figure 3c,g). Alkenone $\delta^{13}C$ values are relatively stable through the Pleistocene portion of the record, varying between -24.5 ‰ and -23.2 ‰. Values are slightly higher in the Pliocene, varying between -24.1 ‰ and -21.7 ‰, *G. ruber* $\delta^{13}C$ values are relatively stable through the whole record, varying between 0.53 ‰ and 1.57 ‰. These give rise to ε_p values which are similarly fairly stable, varying between 10.5 ‰ and 12.2 ‰ in the Pleistocene, and between 9.53 ‰ and 11.8 ‰ in the Pliocene. Our UK37' SST (Figure 3c,g) record shows warmer temperatures in the Pliocene of around 27 °C, with cooler temperatures recorded in the Pleistocene, with the coldest SST recorded in the glacial which is ~2 °C cooler than the interglacial. These record are combined (see Methods) to produce the pCO_2 record (Figure 2, 3c,f) which shows largely stable and invariant values through both the Pliocene and Pleistocene portions of our record. We estimate the 'b' term of equation 1 using the modern day relationship observed between 'b' and $[PO_4^{3-}]$. This term combines all other physiological factors which may influence ε_p including cell size, growth rate and light limitation.

Published low temporal resolution Pliocene records from Site 999 (Seki et al., 2010), using both the $CO_{2(\varepsilon p\text{-}alk)}$ and $CO_{2(\delta 11Bplank)}$ palaeobarometers, show a pCO_2 decrease at ~ 2.8 Ma. However, this agreement relies on correcting the $CO_{2(\varepsilon p\text{-}alk)}$ for changes in haptophyte cell size, which was based on a low temporal resolution lith size record (Seki et al., 2010). Changes in haptophyte cell size alter the volume:surface area ratio available for gaseous exchange, and can therefore modify the fractionation recorded

Clim. Past Discuss., https://doi.org/10.5194/cp-2018-152
Manuscript under review for journal Clim. Past
Discussion started: 7 November 2018

by $CO_{2(\varepsilon p\text{-}alk)}$(Popp et al., 1998). Our new $CO_{2(\varepsilon p\text{-}alk)}$ record at Site 999 now spans 3.3- 2.6 Ma at higher temporal resolution, supplementing data from Badger et al.,(2013b). A lith size record has also been generated for the same samples used for $CO_{2(\varepsilon p\text{-}alk)}$ for 3.3-2.6 Ma (Davis et al., 2013). We find no evidence to support the change in lith size applied by Seki et al., (2010) with lith size (and hence cell size) remaining stable across the primary pCO_2 change at 2.8 Ma (Davis et al., 2013). Consequently, although our new $CO_{2(\varepsilon p\text{-}alk)}$ record is higher resolution than that of Seki et al., (2010), we no longer have any evidence for the cell size shift at 2.7 Ma (Figure 4).

We compare our record with the $CO_{2(\delta 11Bplank)}$ records of Martínez-Botí et al., (2015) in Figure 2. With the cell size correction now removed, the decrease in $CO_{2(\varepsilon p\text{-}alk)}$ across the INHG, and the agreement of $CO_{2(\varepsilon p\text{-}alk)}$ with $CO_{2(\delta 11Bplank)}$, both now disappear (red symbols, Figure 2b). As such, $CO_{2(\varepsilon p\text{-}alk)}$ for the whole of this Pliocene interval (2.6 – 3.3 Ma) remains stable and low (mean $CO_{2\,(\varepsilon p\text{-}alk)}$ =251±13; 1σ min=228 max=286 μatm), whereas $CO_{2(\delta 11Bplank)}$ is on average higher and more variable (mean $CO2_{(\delta 11Bplank)}$=342±50; 1σ min=234 max=452 μatm).

In the Pleistocene, our $CO_{2(\varepsilon p\text{-}alk)}$ record covers one complete glacial-interglacial (G-IG) cycle from 110 – 260 ka, encompassing Marine Isotope Stage (MIS) 5,6,7 the end of MIS 8, and terminations II and III (red open diamonds, Figure 2a). The $CO_{2(\delta 11Bplank)}$ record of Chalk et al. (2017) covers two G-IG cycles from the late Holocene to MIS8 (blue open circles, Figure 2a). $\delta^{11}B_{plank}$ closely tracks the rise and fall of pCO_2 derived from ice cores (Chalk et al., 2017), with $CO_{2(\delta 11Bplank)}$ exhibiting similar values to atmospheric CO_2 within uncertainty (Figure 2a), and with only small deviations from ice core CO_2 as a result of: (*i*) the noise in the reconstruction; and (*ii*) perhaps a small diagenetic effect on $CO_{2(\delta 11Bplank)}$ relating to periods of carbonate dissolution in portions of the core which show high foraminiferal fragmentation (e.g. MIS 5d; Schmidt et al., 2006).

In contrast, $CO_{2(\varepsilon p\text{-}alk)}$ is within error of the ice core data only during the interglacials when CO_2 partial pressures are similar to those of the pre-industrial era. Crucially, $CO_{2(\varepsilon p\text{-}alk)}$ clearly fails to record the lower pCO_2 of the glacials, remaining at around 260 μatm throughout (mean $CO_{2(\varepsilon p\text{-}alk)}$=259±27; Figure 2a). This concentration of pCO_2 is also very close to that recorded by $CO_{2(\varepsilon p\text{-}alk)}$ in the Pliocene at this Site (mean $CO_{2(\varepsilon p\text{-}alk)}$=252±26 μatm; Figure 2). Similar alkenone behaviour has also been observed in another, albeit lower resolution, record from ODP Site 925 (Zhang et al., 2013; Figure 2), where the $CO_{2(\varepsilon p\text{-}alk)}$ remains unchanged during the Pleistocene (20 – 170 Ka) and Pliocene.

Clim. Past Discuss., https://doi.org/10.5194/cp-2018-152
Manuscript under review for journal Clim. Past
Discussion started: 7 November 2018

Overall, these results suggest that, at least at these sites, the $CO_{2(\delta 11Bplank)}$ palaeobarometer does faithfully record atmospheric CO_2 change, whereas the $CO_{2(\varepsilon p\text{-}alk)}$ proxy is unable to reconstruct the low levels of atmospheric CO_2 during the glacial. This suggests that, in its present and frequently applied form, $CO_{2(\varepsilon p\text{-}alk)}$ is not accurately recording atmospheric CO_2, and this could explain the discrepancy between the Pliocene $CO_{2(\varepsilon p\text{-}alk)}$ and $CO_{2(\delta 11Bplank)}$ records. We further evaluate this by using regression analysis between ice core and the paired-proxy data (Figure 5). $CO_{2(\delta 11Bplank)}$ levels are largely consistent with those determined from ice cores, clustering around the 1:1 line with a slope also close to 1 (0.95±0.13) (Figure 5a), whereas variance in $CO_{2(\varepsilon p\text{-}alk)}$ is strongly muted compared to that observed in the ice core data (Figure 5b).

As both cell size (Popp et al., 1998) and growth rate (Bidigare et al., 1997) can modify $\delta^{13}C_{alk}$ via the 'b' term, we investigated whether either of these could explain the muted response of $CO_{2(\varepsilon p\text{-}alk)}$ to atmospheric CO_2. Hapytophyte cell size can be estimated from their lith size, but as noted above, there is no evidence for significant changes in the Pliocene (Davis et al., 2013) nor is there evidence for any change across MIS5-8 (Figure 4a). There is an overall reduction in lith size from the Pliocene to the Pleistocene (Figure 4a, b), which could offset a long term pCO_2 decline and thus explain the apparent lack of difference between Pliocene and Pleistocene $CO_{2(\varepsilon p\text{-}alk)}$ at Site 999. However, this longer-term reduction in lith size cannot explain the muted response to Pleistocene G-IG CO_2 change.

Growth rate is more difficult to reconstruct; most available proxy systems reconstruct phytoplankton or whole ecosystem productivity, rather than coccolithophorid growth rate. However emerging trace metal datasets do suggest changing productivity on glacial-interglacial timescales at Site 999, with lower productivity in the glacial (Trumbo, 2015). If lower productivity is linked with a simultaneous reduction in growth rate, then it could explain some of the lack of signal in $CO_{2(\varepsilon p\text{-}alk)}$.

This suggests that either our understanding of growth rate effects on $CO_{2(\varepsilon p\text{-}alk)}$ is incorrect, or the estimation of cell size using preserved liths does not capture original cell size variations, or a combination of these or other factors leads to the rather muted trends in $CO_{2(\varepsilon p\text{-}alk)}$ through the glacial-interglacial cycle.

Clim. Past Discuss., https://doi.org/10.5194/cp-2018-152
Manuscript under review for journal Clim. Past
Discussion started: 7 November 2018

The failure of $CO_{2(\varepsilon p\text{-}alk)}$ from these two sites to record the G-IG pCO_2 variation also necessitates reassessment of earlier $CO_{2(\varepsilon p\text{-}alk)}$ studies that were able to reconstruct such changes. For instance Jasper and Hayes, (1990) replicated the CO_2 change over the last 100 kyrs of the Vostok ice core from DSDP Site 619 (Gulf of Mexico; Figure 1,6). However, a record from the Equatorial Pacific (MANOP site C; Figure 1, 6) also failed to replicate the pCO_2 changes observed in the ice core data over the last 255 kyrs, and instead was interpreted as recording changes in air-sea equilibrium, not atmospheric CO_2 (Jasper et al., 1994). Smoothing and correction for estimated growth rates revealed the gross features of the ice core record (Stoll and Schrag, 2000), but still only recorded 30-35 % of the variance in the ice core data (Bereiter et al., 2015; Stoll and Schrag, 2000). These two studies interpreted their data using a different ε_p relationship than later work; when these data are recalculated using the more recent model the patterns remain unchanged (Figure 6). What is more, in a global alkenone $\delta^{13}C$ calibration study (Pagani et al., 2002) aimed at replicating Holocene atmospheric conditions it was noted that low latitude (sub-tropical) sites perform poorly, consistent with our observations. Considering this present study and previously published work, 3 out of 4 late Pleistocene alkenone $\delta^{13}C$ studies do not show the variations in pCO_2 evident from contemporaneous ice core records (Figure 2; Figure 6).

Our Bayesian approach allows us to explore the $CO_{2(\varepsilon p\text{-}alk)}$ proxy, as it was mathematically expressed by Bidigare et al (1997) and subsequent authors, and what variables may be responsible for causing the observed disagreements with the ice core and $CO_{2(\delta 11Bplank)}$ records given a largely invariant ε_p. Figure 7 illustrates the prior distributions of the input variables (blue) and an example posterior for the alkenone sample at 150 kyr (red). As can be seen in this example, selecting only those simulations of $CO_{2(\varepsilon p\text{-}alk)}$ that overlap with the ice core CO_2 for this time interval shifts the distributions such that an agreement is found when b is lower than the prior, ε_f tends to be higher than the prior and SST and CO_2 disequilibrium are little different. Figure 8 shows the posterior median and 95 % distribution of b, ε_f and SST for all the samples from the Pleistocene and Pliocene in time series. Patterns that emerge are illustrated in Figure 9, where a negative relationship between pCO_2 and posterior ε_f and a positive relationship between pCO_2 and posterior b and SST is evident. For SST it should also be noted that for the Pleistocene the posterior correlates well with the prior, while for the Pliocene it is significantly elevated (Figure 9), perhaps suggesting a role for incorrect SST in driving some of the lack of Pliocene to Pleistocene change in $CO_{2(\varepsilon p\text{-}alk)}$ observed (Figure 2).

Clim. Past Discuss., https://doi.org/10.5194/cp-2018-152
Manuscript under review for journal Clim. Past
Discussion started: 7 November 2018

We recognize that the nature of the patterns we observe here is a function somewhat of the range used for each input term. The chosen ranges are however conservative, but realistic, assessments of the likely uncertainty associated with each term. For instance, b ± 40 encompasses the residual scatter around the relationship between b and [PO_4] described by Pagani et al., (2005). In addition to pointing towards a potential underestimate of Pliocene SST with the U^{K}_{37}' proxy at ODP 999, this Bayesian treatment supports the assertion that the current understanding of the $CO_{2(\varepsilon p\text{-}alk)}$ proxy is wanting. In particular, it appears that the physiological parameters packaged in the b-term, and potentially the degree of fractionation upon fixation, ε_f, are themselves a function of CO_2 or some parameter that correlates with CO_2 (e.g. temperature, nutrients, growth rate etc.).

An alternative explanation however could be that the invariant parameterisation of physiological factors into the 'b' term-model could be flawed or at least lacking important components. The dominant species producing alkenones in this part of the Caribbean today, and likely since its first appearance 290 kyrs ago, is *Emiliania huxleyi* (Winter et al., 2002). Recent experimental work has shown that this globally important species has evolved a carbon concentrating mechanism (CCM) to respond to limiting CO_2 by upregulating genes at low DIC to maintain carbon requirements (Bach et al., 2013). CCMs result in a breakdown of the relationship between ε_p and CO_2 as defined and calibrated by Bidigare et al., (1997). It has been thought that the increased expression of CCMs will cause ε_p values to decrease, due to the isotopic offset between $CO_{2(aq)}$ and HCO_3^- and decreased carbon leakage from the cell (Zhang et al., 2013), effectively exacerbating the expected trend towards lower ε_p values at lower pCO_2 and inconsistent with our observation of relatively stable ε_p values across G-IG cycles. However, CCMs appear to modulate carbon flow across cellular compartments (e.g. cytosol, chloroplast and calcification vesicle), and could also yield elevated rather than lower ε_p due to the concentrating of CO_2 at the site of carbon fixation (Bolton and Stoll, 2013). Additionally, CO_2 optima are species specific and vary with temperature which may explain why some sites in the region are capable of recording G-IG changes, as temperature modulates resource allocation between biosynthesis and photosynthesis (Sett et al., 2014). Furthermore, it has been postulated that changes in carbonate chemistry affect the redox state inside *E. huxleyi* cells which subsequently causes a reorganization of carbon flux within and across cellular compartments (Rokitta et al., 2012). Such a re-distribution of inorganic carbon amongst different pathways also likely influences ε_p and is currently not mechanistically represented by Bidigare et al., (1997) and other models.

Clim. Past Discuss., https://doi.org/10.5194/cp-2018-152
Manuscript under review for journal Clim. Past
Discussion started: 7 November 2018

4. Conclusions

Our data show that the classical application of the alkenone pCO_2 proxy fails to capture glacial-interglacial changes observed in the ice cores. With increased confidence in $CO_{2(\delta 11Bplank)}$ supplied by that proxy's ability to capture Pleistocene pCO_2 variability, our data also suggest that the discrepancy between $CO_{2(\delta 11Bplank)}$- and $CO_{2(\varepsilon p\text{-}alk)}$ in the Pliocene may also be due to problems with $CO_{2(\varepsilon p\text{-}alk)}$. Emerging insights into coccolithophore CO_2 allocation pathways and their sensitivity to CO_2 and temperature, in conjunction with our inter-proxy comparisons, indicate that the long-standing $CO_{2(\varepsilon p\text{-}alk)}$ proxy requires major revision and recalibration. If CCMs are preferentially more important for the alkenone palaeobarometer than growth rate, the muted alkenone palaeobarometer response may be limited to the low CO_2 world of the Plio-Pleistocene and particularly in tropical waters where $CO_{2[aq]}$ is especially low. By extension, this proxy (and interpretations based on it) likely retains utility at the higher CO_2 levels typical of the early Cenozoic (and at high latitudes where $CO_{2[aq]}$ is high) where active carbon uptake is less likely (Zhang et al., 2013). This is especially true if haptophyte CCMs only evolved in the late Miocene as a response to declining CO_2 levels (Bolton and Stoll, 2013). Regardless, the discrepancy between $CO_{2(\varepsilon p\text{-}alk)}$ and ice core CO_2 records indicates that alkenone isotopes in several locations do not faithfully record atmospheric CO_2 at relatively low, Plio-Pleistocene-like CO_2 levels. Furthermore, the muted response of $CO_{2(\varepsilon p\text{-}alk)}$ to $[CO_{2(aq)}]$ at lower concentrations calls into question the underlying basis of the high climate sensitivities previously reconstructed using this method in the Plio-Pleistocene (Pagani et al., 2009). This, coupled with further evidence of the fidelity of $CO_{2(\delta 11Bplank)}$ at Site 999 suggests that the climate sensitivities derived from $CO_{2(\delta 11Bplank)}$ (which are consistent with climate models used both in palaeoclimate and future climate projections) are more accurate (Martínez-Botí et al., 2015b).

Author contributions

MPSB and GLF conceived the study [conceptualization], MPSB, TBC and GLF designed the methodology, carried out data collection and analysed the data [formal analysis, investigation, methodology]. PRB, SJG, HP and AM performed data collection, PFS finalised the age model [investigation]. MPSB wrote the manuscript and prepared figures [Visualisation, Writing – original draft]. RDP (PI) and GLF and DNS (CoIs) supervised the project and acquired funding [Funding acquisition & Supervision]. All authors contributed to interpretation, writing and reviewing the manuscript [Writing – review & editing].

Acknowledgements

This study used samples provided by the International Ocean Discovery Program (IODP). We thank Alex Hull and Gemma Bowler for laboratory work, Lisa Schönborn and Günter Meyer for technical assistance, Alison Kuhl and Ian Bull for research support, and Andy Milton at the University of Southampton for maintaining some of the mass spectrometers used in this study. This study was funded by NERC grant NE/H006273/1 to RDP, DNS and GLF (which supported MPSB). We also acknowledge the ERC Award T-GRES and a Royal Society Wolfson Research Merit Award to RDP. We thank Kirsty Edgar for comments on an early draft of the manuscript and reviewers through various rounds of review whose comments greatly improved the manuscript.

References

Ahn, J., Brook, E. J., Mitchell, L., Rosen, J., McConnell, J. R., Taylor, K., Etheridge, D. and Rubino, M.: Atmospheric CO2 over the last 1000 years: A high-resolution record from the West Antarctic Ice Sheet (WAIS) Divide ice core, Global Biogeochem. Cycles, 26(2), n/a-n/a, doi:10.1029/2011GB004247, 2012.

Anagnostou, E., John, E. H., Edgar, K. M., Foster, G. L., Ridgwell, A., Inglis, G. N., Pancost, R. D., Lunt, D. J. and Pearson, P. N.: Changing atmospheric CO2 concentration was the primary driver of early Cenozoic climate, Nature, 533(7603), 380–384, doi:10.1038/nature17423, 2016.

Bach, L. T., Mackinder, L. C. M., Schulz, K. G., Wheeler, G., Schroeder, D. C., Brownlee, C. and Riebesell, U.: Dissecting the impact of CO2 and pH on the mechanisms of photosynthesis and calcification in the coccolithophore Emiliania huxleyi.,

New Phytol., 199(1), 121–34, doi:10.1111/nph.12225, 2013.

Badger, M. P. S., Lear, C. H., Pancost, R. D., Foster, G. L., Bailey, T. R., Leng, M. J. and Abels, H. a.: CO2 drawdown following the middle Miocene expansion of the Antarctic Ice Sheet, Paleoceanography, 28, 42–53, doi:10.1002/palo.20015, 2013a.

Badger, M. P. S., Schmidt, D. N., Mackensen, A. and Pancost, R. D.: High-resolution alkenone palaeobarometry indicates relatively stable pCO(2) during the Pliocene (3.3-2.8 Ma)., Philos. Trans. A. Math. Phys. Eng. Sci., 371, 20130094, doi:10.1098/rsta.2013.0094, 2013b.

Bartoli, G., Hönisch, B. and Zeebe, R. E.: Atmospheric CO 2 decline during the Pliocene intensification of Northern Hemisphere glaciations, Paleoceanography, 26(4), n/a-n/a, doi:10.1029/2010PA002055, 2011.

Bereiter, B., Eggleston, S., Schmitt, J., Nehrbass-Ahles, C., Stocker, T. F., Fischer, H., Kipfstuhl, S. and Chappellaz, J.: Revision of the EPICA Dome C CO 2 record from 800 to 600 kyr before present, Geophys. Res. Lett., 42(2), 542–549, doi:10.1002/2014GL061957, 2015.

Bidigare, R., Fluegge, A., Freeman, K. H., Hanson, K., Hayes, J. M., Hollander, D., Jasper, J. P., King, L. L., Laws, E., Milder, J., Millero, F. J., Pancost, R., Popp, B. N., Steinberg, P. and Wakeham, S. G.: Consistent fractionation of 13C in nature and in the laboratory: Growth-rate effects in some haptophyte algae, Global Biogeochem. Cycles, 11(2), 279–292 [online] Available from: http://onlinelibrary.wiley.com/doi/10.1029/96GB03939/full (Accessed 12 January 2015), 1997.

Bolton, C. T. and Stoll, H. M.: Late Miocene threshold response of marine algae to carbon dioxide limitation., Nature, 500(7464), 558–62, doi:10.1038/nature12448, 2013.

Chalk, T. B., Hain, M. P., Foster, G. L., Rohling, E. J., Sexton, P. F., Badger, M. P. S., Cherry, S. G., Hasenfratz, A. P., Haug, G. H., Jaccard, S. L., Martínez-García, A., Pälike, H., Pancost, R. D. and Wilson, P. A.: Causes of ice age intensification across the Mid-Pleistocene Transition, Proc. Natl. Acad. Sci., 201702143, doi:10.1073/pnas.1702143114, 2017.

Davis, C. V., Badger, M. P. S., Bown, P. R. and Schmidt, D. N.: The response of calcifying plankton to climate change in the Pliocene, Biogeosciences, 10, 6131–6139, doi:10.5194/bg-10-6131-2013, 2013.

Delaney, M. L. and Boyle, E. A.: Li, Sr, Mg, and Na in foraminiferal calcite shells from laboratory culture , sediment traps, and sediment cores, Geochim. Cosmochim. Acta, 49(October 1983), 1327–1341, 1985.

Dickson, A. G.: Thermodynamics of the dissociation of boric acid in synthetic seawater from 273.15 to 318.15 K, Deep Sea Res. Part A. Oceanogr. Res. Pap., 37(5), 755–766, doi:10.1016/0198-0149(90)90004-F, 1990.

Evans, D. and Müller, W.: Deep time foraminifera Mg/Ca paleothermometry: Nonlinear correction for secular change in seawater Mg/Ca, Paleoceanography, 27(4), n/a-n/a, doi:10.1029/2012PA002315, 2012.

Foster, G. L.: Seawater pH, pCO2 and [CO2−3] variations in the Caribbean Sea over the last 130 kyr: A boron isotope and

B/Ca study of planktic foraminifera, Earth Planet. Sci. Lett., 271(1–4), 254–266, doi:10.1016/j.epsl.2008.04.015, 2008.

Foster, G. L. and Sexton, P. F.: Enhanced carbon dioxide outgassing from the eastern equatorial Atlantic during the last glacial, Geology, 42(11), 1003–1006, doi:10.1130/G35806.1, 2014.

Foster, G. L., Hönisch, B., Paris, G., Dwyer, G. S., Rae, J. W. B., Elliott, T., Gaillardet, J., Hemming, N. G., Louvat, P. and Vengosh, A.: Interlaboratory comparison of boron isotope analyses of boric acid, seawater and marine CaCO3 by MC-ICPMS and NTIMS, Chem. Geol., 358, 1–14, doi:10.1016/j.chemgeo.2013.08.027, 2013.

Gattuso, J.-P., Epitalalon, J.-M. and Lavigne, H.: Seacarb: Seawater Carbonate Chemistry. R package version 3.0.8, 2015.

Gibbs, S. J., Poulton, A. J., Bown, P. R., Daniels, C. J., Hopkins, J., Young, J. R., Jones, H. L., Thiemann, G. J., O'Dea, S. A. and Newsam, C.: Species-specific growth response of coccolithophores to Palaeocene–Eocene environmental change, Nat. Geosci., 6(3), 218–222, doi:10.1038/ngeo1719, 2013.

Hemming, N. G. and Hanson, G. N.: Boron isotopic composition and concentration in modern marine carbonates, Geochim. Cosmochim. Acta, 56(1), 537–543, doi:10.1016/0016-7037(92)90151-8, 1992.

Henderiks, J.: Coccolithophore size rules — Reconstructing ancient cell geometry and cellular calcite quota from fossil coccoliths, Mar. Micropaleontol., 67(1–2), 143–154, doi:10.1016/j.marmicro.2008.01.005, 2008.

Henehan, M. J., Rae, J. W. B., Foster, G. L., Erez, J., Prentice, K. C., Kucera, M., Bostock, H. C., Martínez-Botí, M. A., Milton, J. A., Wilson, P. A., Marshall, B. J. and Elliott, T.: Calibration of the boron isotope proxy in the planktonic foraminifera Globigerinoides ruber for use in palaeo-CO2 reconstruction, Earth Planet. Sci. Lett., 364, 111–122, doi:10.1016/j.epsl.2012.12.029, 2013.

Hönisch, B. and Hemming, N. G.: Surface ocean pH response to variations in pCO2 through two full glacial cycles, Earth Planet. Sci. Lett., 236(1–2), 305–314, doi:10.1016/j.epsl.2005.04.027, 2005.

Jasper, J. and Hayes, J.: A carbon isotope record of CO2 levels during the late Quaternary, Nature, 347, 462–464 [online] Available from: http://www.nature.com/nature/journal/v347/n6292/abs/347462a0.html (Accessed 12 January 2015), 1990.

Jasper, J., Hayes, J., Mix, A. and Prahl, F.: Photosynthetic fractionation of 13C and concentrations of dissolved CO2 in the central equatorial Pacific during the last 255,000 years, Paleoceanography, 9(6), 781–798 [online] Available from: http://onlinelibrary.wiley.com/doi/10.1029/94PA02116/full (Accessed 12 January 2015), 1994.

Klochko, K., Kaufman, A. J., Yao, W., Byrne, R. H. and Tossell, J. A.: Experimental measurement of boron isotope fractionation in seawater, Earth Planet. Sci. Lett., 248(1–2), 276–285, doi:10.1016/j.epsl.2006.05.034, 2006.

Lacis, A. A., Schmidt, G. A., Rind, D. and Ruedy, R. A.: Atmospheric CO2: Principal Control Knob Governing Earth's Temperature, Science (80-.)., 330(6002), 356–359, doi:10.1126/science.1190653, 2010.

Laws, E. a., Bidigare, R. R. and Popp, B. N.: Effect of growth rate and CO2 concentration on carbon isotopic fractionation by

the marine diatom Phaeodactylum tricornutum, Limnol. Oceanogr., 42(7), 1552–1560, doi:10.4319/lo.1997.42.7.1552, 1997.

Lisiecki, L. E. and Raymo, M. E.: A Pliocene-Pleistocene stack of 57 globally distributed benthic δ 18 O records, Paleoceanography, 20(1), n/a-n/a, doi:10.1029/2004PA001071, 2005.

Martínez-Botí, M. A., Foster, G. L., Chalk, T. B., Rohling, E. J., Sexton, P. F., Lunt, D. J., Pancost, R. D., Badger, M. P. S. and Schmidt, D. N.: Plio-Pleistocene climate sensitivity evaluated using high-resolution CO<inf>2</inf> records, Nature, 518(7537), doi:10.1038/nature14145, 2015a.

Martínez-Botí, M. A., Foster, G. L., Chalk, T. B., Rohling, E. J., Sexton, P. F., Lunt, D. J., Pancost, R. D., Badger, M. P. S. and Schmidt, D. N.: Plio-Pleistocene climate sensitivity evaluated using high-resolution CO2 records, Nature, 518(7537), 49–54, doi:10.1038/nature14145, 2015b.

Pagani, M., Freeman, K. H., Ohkouchi, N. and Caldeira, K.: Comparison of water column [CO 2aq] with sedimentary alkenone-based estimates: A test of the alkenone-CO 2 proxy, Paleoceanography, 17(4), 21-1-21–12, doi:10.1029/2002PA000756, 2002.

Pagani, M., Zachos, J. C., Freeman, K. H., Tipple, B. and Bohaty, S.: Marked Decline in Atmospheric Carbon Dioxide Concentrations During the Paleogene, Science (80-.)., 309(July), 600–603, 2005.

Pagani, M., Liu, Z., LaRiviere, J. and Ravelo, A. C.: High Earth-system climate sensitivity determined from Pliocene carbon dioxide concentrations, Nat. Geosci., 3(1), 27–30, doi:10.1038/ngeo724, 2009.

Pagani, M., Huber, M., Liu, Z., Bohaty, S. M., Henderiks, J., Sijp, W., Krishnan, S. and DeConto, R. M.: The role of carbon dioxide during the onset of Antarctic glaciation., Science, 334(6060), 1261–4, doi:10.1126/science.1203909, 2011.

Paillard, D., Labeyrie, L. and Yiou, P.: Macintosh Program performs time-series analysis, Eos, Trans. Am. Geophys. Union, 77(39), 379–379, doi:10.1029/96EO00259, 1996.

PALAEOSENS: Making sense of palaeoclimate sensitivity., Nature, 491(7426), 683–91, doi:10.1038/nature11574, 2012.

Pearson, P. N., Foster, G. L. and Wade, B. S.: Atmospheric carbon dioxide through the Eocene-Oligocene climate transition., Nature, 461(7267), 1110–3, doi:10.1038/nature08447, 2009.

Petit, J., Jouzel, J., Raynaud, D., Barkov, N., Barnola, J.-M., Basile, I., Bender, M., Chappellaz, J., Davis, M., Delaygue, G., Delmotte, M., Kotlyakov, V., Legrand, M., Lipenkov, V., Lorius, C., Pepin, K., Ritz, C., Saltzman, E. and Stievenard, M.: Climate and atmospheric history of the past 420,000 years from the Vostok ice core, Antarctica, Nature, 399, 429–436 [online] Available from: http://www.nature.com/nature/journal/v399/n6735/abs/399429a0.html (Accessed 12 January 2015), 1999.

Popp, B., Laws, E., Bidigare, R., Dore, J., Hanson, K. and Wakeham, S. G.: Effect of phytoplankton cell geometry on carbon isotopic fractionation, Geochim. Cosmochim. Acta, 62(1), 67–77 [online] Available from: http://www.sciencedirect.com/science/article/pii/S0016703797003335 (Accessed 12 January 2015), 1998.

Rae, J. W. B., Foster, G. L., Schmidt, D. N. and Elliott, T.: Boron isotopes and B/Ca in benthic foraminifera: Proxies for the deep ocean carbonate system, Earth Planet. Sci. Lett., 302(3–4), 403–413, doi:10.1016/j.epsl.2010.12.034, 2011.

Rokitta, S. D., John, U. and Rost, B.: Ocean Acidification Affects Redox-Balance and Ion-Homeostasis in the Life-Cycle Stages of Emiliania huxleyi, edited by S. Dupont, PLoS One, 7(12), e52212, doi:10.1371/journal.pone.0052212, 2012.

Sanyal, A. and Hemming, N.: Oceanic pH control on the boron isotopic composition of foraminifera: evidence from culture experiments, Paleoceanography, 11(5), 513–517 [online] Available from: http://onlinelibrary.wiley.com/doi/10.1029/96PA01858/full (Accessed 12 January 2015), 1996.

Sanyal, A., Hemming, N., Hanson, G. and Broecker, W.: Evidence for a higher pH in the glacial ocean from boron isotopes in foraminifera, Nature, 373, 234–236 [online] Available from: http://www.pmc.ucsc.edu/~apaytan/290A_Winter2014/pdfs/B isotopes Jn 24-1.pdf (Accessed 12 January 2015), 1995.

Schmidt, M. W., Vautravers, M. J. and Spero, H. J.: Western Caribbean sea surface temperatures during the late Quaternary, Geochemistry, Geophys. Geosystems, 7(2), n/a-n/a, doi:10.1029/2005GC000957, 2006.

Seki, O., Foster, G. L., Schmidt, D. N., Mackensen, A., Kawamura, K. and Pancost, R. D.: Alkenone and boron-based Pliocene pCO2 records, Earth Planet. Sci. Lett., 292(1–2), 201–211, doi:10.1016/j.epsl.2010.01.037, 2010.

Sett, S., Bach, L. T., Schulz, K. G., Koch-Klavsen, S., Lebrato, M. and Riebesell, U.: Temperature modulates coccolithophorid sensitivity of growth, photosynthesis and calcification to increasing seawater pCO_2., PLoS One, 9(2), e88308, doi:10.1371/journal.pone.0088308, 2014.

Sheward, R. M., Poulton, A. J., Gibbs, S. J., Daniels, C. J. and Bown, P. R.: Physiology regulates the relationship between coccosphere geometry and growth phase in coccolithophores, Biogeosciences, 14(6), 1493–1509, doi:10.5194/bg-14-1493-2017, 2017.

Sosdian, S. M., Greenop, R., Hain, M. P., Foster, G. L., Pearson, P. N. and Lear, C. H.: Constraining the evolution of Neogene ocean carbonate chemistry using the boron isotope pH proxy, Earth Planet. Sci. Lett., 498, 362–376, doi:10.1016/J.EPSL.2018.06.017, 2018.

Stoll, H. M. and Schrag, D. P.: Coccolith Sr/Ca as a new indicator of coccolithophorid calcification and growth rate, Geochemistry, Geophys. Geosystems, 1(5), n/a-n/a, doi:10.1029/1999GC000015, 2000.

Super, J. R., Thomas, E., Pagani, M., Huber, M., Brien, C. O. and Hull, P. M.: North Atlantic temperature and pCO2 coupling in the early-middle Miocene, Geology, 46(6), 519–522, doi:https://doi.org/10.1130/G40228.1, 2018.

Takahashi, T., Sutherland, S. C., Wanninkhof, R., Sweeney, C., Feely, R. a., Chipman, D. W., Hales, B., Friederich, G., Chavez, F., Sabine, C., Watson, A., Bakker, D. C. E., Schuster, U., Metzl, N., Yoshikawa-Inoue, H., Ishii, M., Midorikawa, T., Nojiri, Y., Körtzinger, A., Steinhoff, T., Hoppema, M., Olafsson, J., Arnarson, T. S., Tilbrook, B., Johannessen, T., Olsen, A., Bellerby, R., Wong, C. S., Delille, B., Bates, N. R. and de Baar, H. J. W.: Climatological mean and decadal change in

surface ocean pCO2, and net sea–air CO2 flux over the global oceans, Deep Sea Res. Part II Top. Stud. Oceanogr., 56(8–10), 554–577, doi:10.1016/j.dsr2.2008.12.009, 2009.

Team, R. C.: R: A language and environment for statistical computing, 2015.

Trumbo, S. K.: Marine Export Productivity and the Demise of the Central American Seaway, UC San Diego. [online] Available from: http://www.escholarship.org/uc/item/83f2w736, 2015.

Winter, A., Rost, B., Hilbrecht, H. and Elbrächter, M.: Vertical and horizontal distribution of coccolithophores in the Caribbean Sea, Geo-Marine Lett., 22(3), 150–161, doi:10.1007/s00367-002-0108-8, 2002.

YOUNG, J.: Size variation of Neogene Reticulofenestra coccoliths from Indian Ocean DSDP Cores, J. Micropalaeontology, 9(1), 71–85, doi:10.1144/jm.9.1.71, 1990.

Zhang, Y. G., Pagani, M., Liu, Z., Bohaty, S. M. and Deconto, R.: A 40-million-year history of atmospheric CO(2)., Philos. Trans. A. Math. Phys. Eng. Sci., 371(2001), 20130096, doi:10.1098/rsta.2013.0096, 2013.

Clim. Past Discuss., https://doi.org/10.5194/cp-2018-152
Manuscript under review for journal Clim. Past
Discussion started: 7 November 2018

Climate of the Past Discussions
Open Access
EGU

Figures

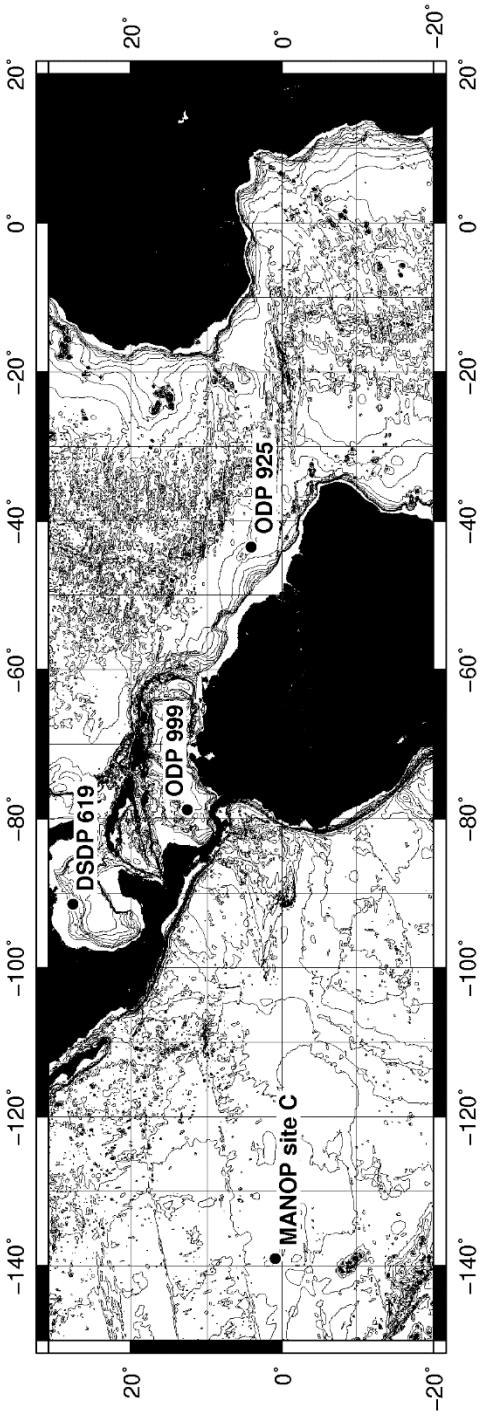

Figure 1 Site map. Locations of sites discussed the text.

Clim. Past Discuss., https://doi.org/10.5194/cp-2018-152
Manuscript under review for journal Clim. Past
Discussion started: 7 November 2018

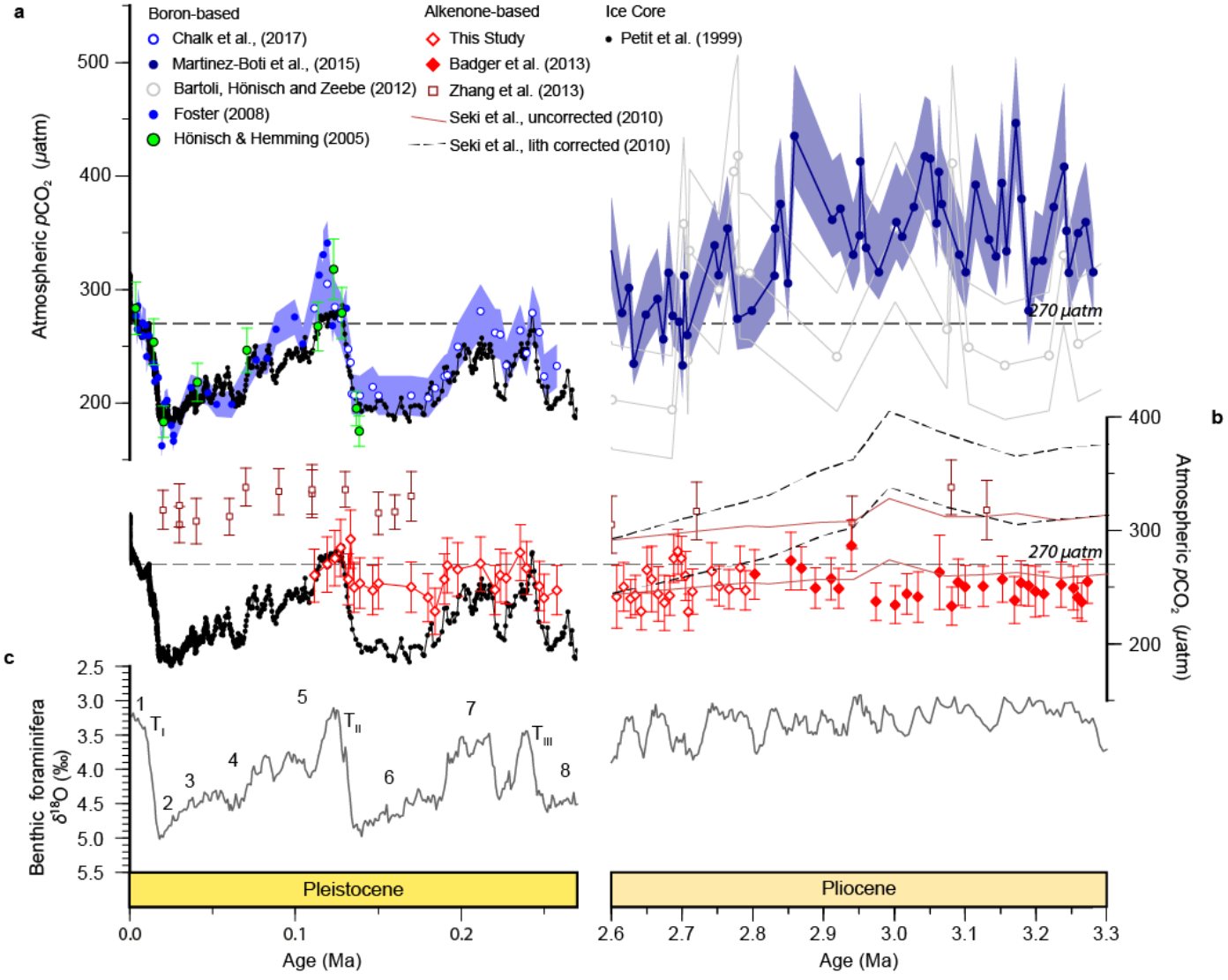

Clim. Past Discuss., https://doi.org/10.5194/cp-2018-152
Manuscript under review for journal Clim. Past
Discussion started: 7 November 2018

Climate of the Past Discussions

Figure 2 Atmospheric CO_2 reconstructions through the Plio-Pleistocene. a: Published boron isotope $CO_{2(\delta 11Bplank)}$ records from ODP Site 999 (open blue circles; (Chalk et al., 2017)**, bright blue filled circles; (Foster, 2008 recalculated as described in the text), grey open circles** (Bartoli et al., 2011)**, dark blue filled circles** (Martínez-Botí et al., 2015b)**) and DSDP Site 668 (green filled circles** (Hönisch and Hemming, 2005)**); b: published $CO_{2(\varepsilon p\text{-}alk)}$ records from ODP Site 925 (maroon open squares** (Zhang et al., 2013)**) and ODP Site 999 (red filled diamonds**(Badger et al., 2013a) **and ice core records (black filled squares** (Bereiter et al., 2015; Petit et al., 1999)**), as well as our new alkenone isotope records from ODP Site 999 (red open diamonds). The lith-size corrected (black dashed envelope) and uncorrected (red solid envelope) of Seki et al., (2010) are also shown. All records are shown with 1σ uncertainties as described elsewhere. c: benthic foraminiferal stable oxygen isotope stack** (Lisiecki and Raymo, 2005) **with Marine Isotope Stages (MIS; numerals) and Terminations (T) indicated.**

Clim. Past Discuss., https://doi.org/10.5194/cp-2018-152
Manuscript under review for journal Clim. Past
Discussion started: 7 November 2018

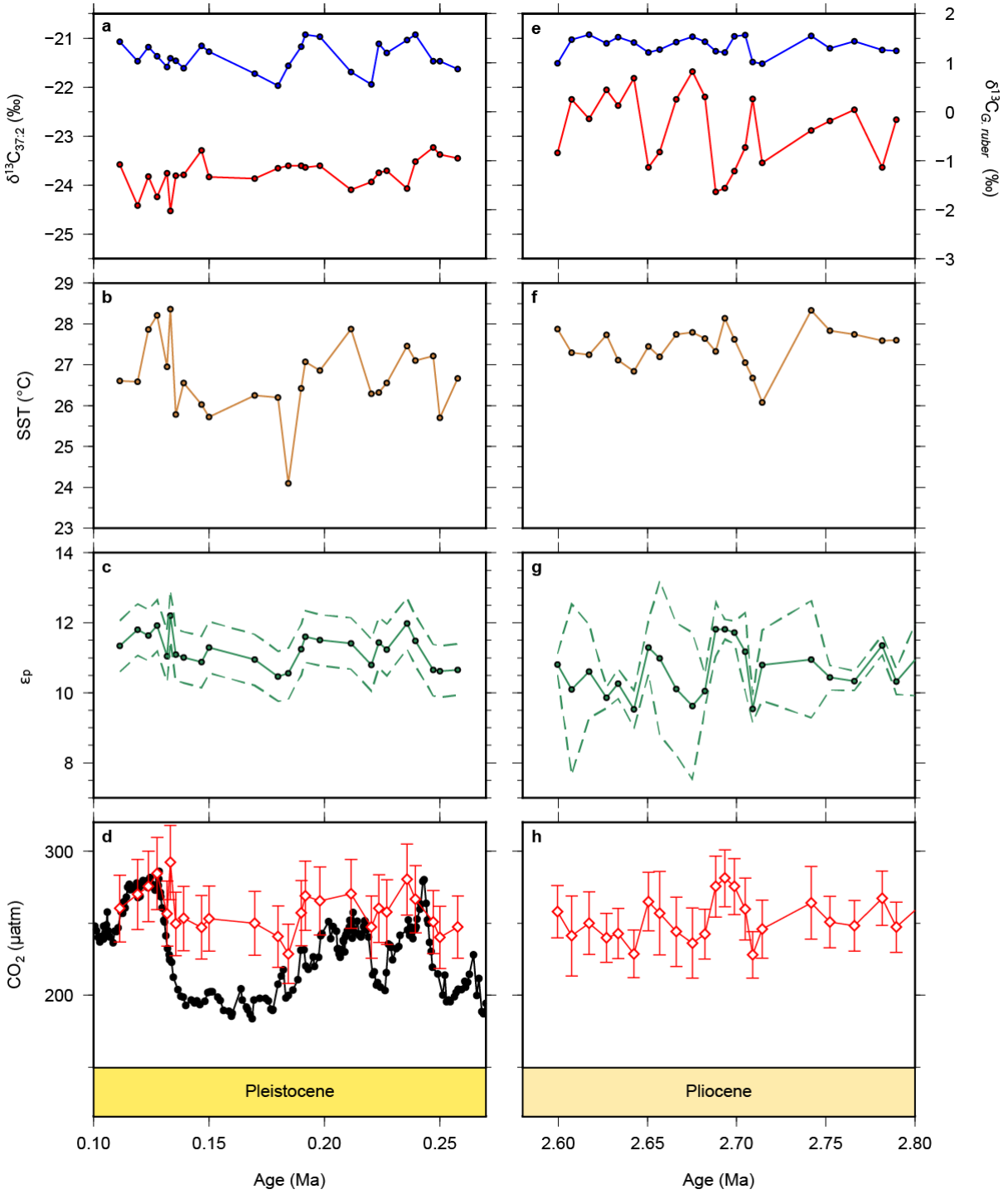

Figure 3 New and recalculated date for $CO_{2(\varepsilon p\text{-}alk)}$ for the Pleistocene and Pliocene from ODP Site 999. Alkenone $\delta^{13}C$ values are shown as red circles for the Pleistocene (a) and Pliocene (b) with *G. ruber* $\delta^{13}C$ from the same samples shown in blue. Alkenone unsaturation-derived SST is shown for the Pleistocene (b) and Pliocene (f). The Pliocene SST data has been previously published as

Clim. Past Discuss., https://doi.org/10.5194/cp-2018-152
Manuscript under review for journal Clim. Past
Discussion started: 7 November 2018

Climate of the Past Discussions
Open Access
EGU

Davis et al., 2013 and is from the same samples as our alkenone $\delta^{13}C$ values. Calculated ε_p data for the Pleistocene (c) and Pliocene (g) and atmospheric pCO_2 from $CO_{2(\varepsilon p\text{-}alk)}$ for the Pleistocene (d) and Pliocene (h) (red diamonds). Ice core pCO_2 data is shown for the Pleistocene (black circles) for comparison (Bereiter et al., 2015)**.**

Clim. Past Discuss., https://doi.org/10.5194/cp-2018-152
Manuscript under review for journal Clim. Past
Discussion started: 7 November 2018

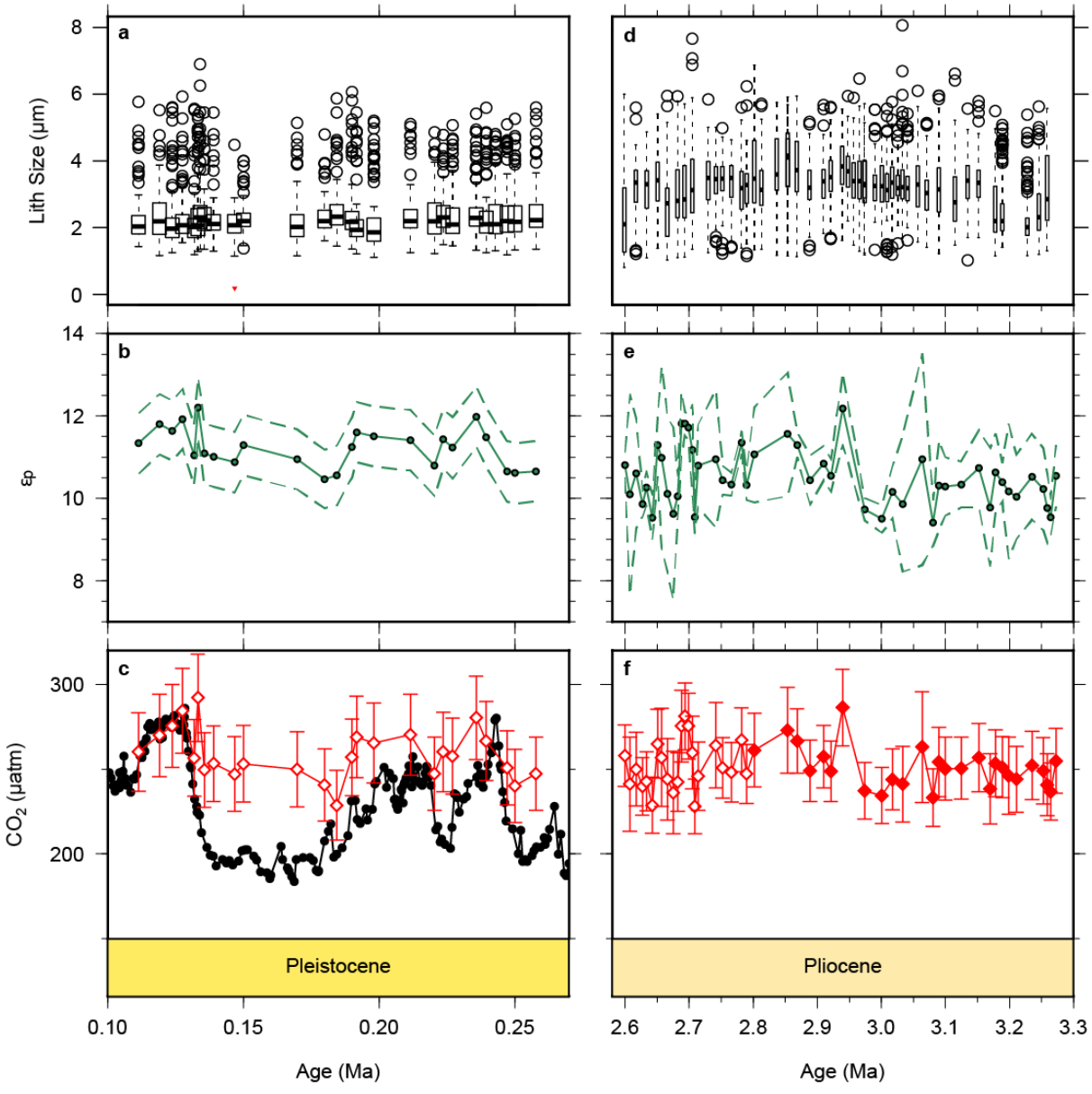

Figure 4 Lith Size data for samples used for CO_2 calculations. Pleistocene lith size (b) are from this study, whilst Pliocene values were published previously (Davis et al., 2013) **but are from the same samples as our CO_2 estimates. Pleistocene ε_p (b) are from this study, whilst the Pliocene data is from this study (2.6-2.8 Mar) and for** Badger et al., (2013b) **(2.8-3.3 Ma). The lower panels show $CO_{2(\varepsilon p\text{-}alk)}$ for the Plesistocene (c) and Pliocene (f) as red diamonds. The filled diamonds in (f) are** (Badger et al., 2013b)**. The Pleistocene ice core data** (Bereiter et al., 2015) **are shown for comparison in (c). The drop in lith size from the Pliocene to Pleistocene is similar to what has been documented previously** (YOUNG, 1990)**. Outliers in a and d were calculated following the 1.5 rule in R (R Core Team, 2015).**

Clim. Past Discuss., https://doi.org/10.5194/cp-2018-152
Manuscript under review for journal Clim. Past
Discussion started: 7 November 2018

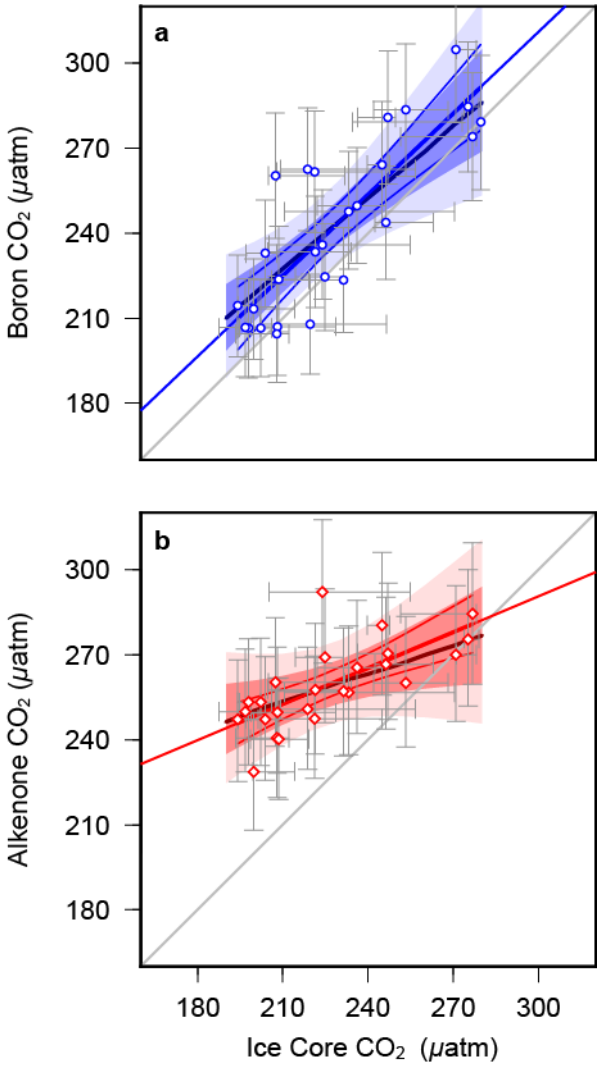

Clim. Past Discuss., https://doi.org/10.5194/cp-2018-152
Manuscript under review for journal Clim. Past
Discussion started: 7 November 2018

Climate of the Past Discussions
Open Access
EGU

Figure 5 Regression analyses of proxy-based pCO2 with ice core data a; $CO_{2(\delta 11Bplank)}$ (Chalk et al., 2017) **and b; $CO_{2(\varepsilon p\text{-}alk)}$ vs ice core data** (Bereiter et al., 2015) **for MIS5-8, interpolated in the age domain. Regression lines (in red/blue) are linear fits with 68 and 95 % confidence intervals, calculated by bootstrapping the uncertainties in proxy *p*CO_2 (Monte Carlo method described in methods). Uncertainty in the ice core values are by estimated by applying a 3000 uncertainty in the age model during interpolation. Uncertainty envelopes considering data points alone (no bootstrap) are solid lines, with pmax regressions in the thicker, darker colours. A 1:1 line is shown in grey for comparison. Statistical calculations were performed in R (R Core Team, 2015).**

Clim. Past Discuss., https://doi.org/10.5194/cp-2018-152
Manuscript under review for journal Clim. Past
Discussion started: 7 November 2018

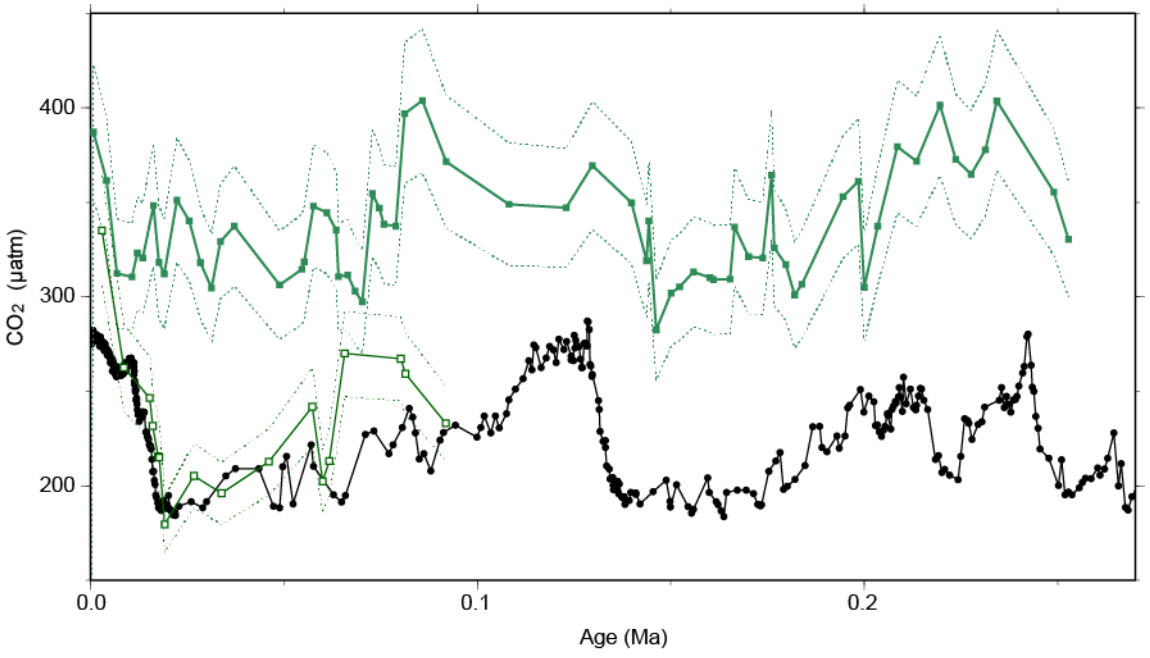

Figure 6 Recalculated $CO_{2(\varepsilon p\text{-}alk)}$. Previous work (Jasper et al., 1994; Jasper and Hayes, 1990) **calculated $CO_{2(\varepsilon p\text{-}alk)}$ using a different model; here we recalculate the earlier work using the modern methodology and Monte Carlo propagation applied to our other sites. MANOP Site C from the central equatorial Pacific (0° 57.2' N, 138° 57.3 W) is shown as green filled squares, DSDP Site 619 in the Pigmy Basin, northern Gulf of Mexico (27° 11.6'N, 91°24.5'W) is shown as open squares, and ice core data are shown as filled black circles and lines** (Bereiter et al., 2015)**. Dashed lines are 2σ uncertainties are from Monte Carlo error propagation as described elsewhere in the text. Neither coccolith nor growth rate corrections were applied.**

Clim. Past Discuss., https://doi.org/10.5194/cp-2018-152
Manuscript under review for journal Clim. Past
Discussion started: 7 November 2018

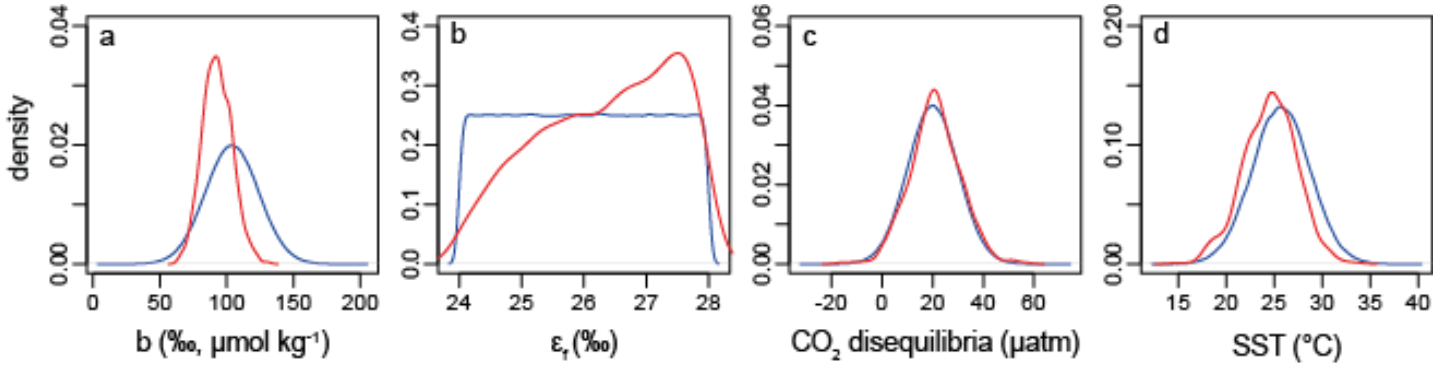

Figure 7. Example of the Bayesian treatment of the $CO_{2(\varepsilon p\text{-}alk)}$ proxy, the sample shown is 0.15 Ma from ODP Site 999. In all panels the prior is shown in blue and the posterior in red. (a) the b-term, (b) ε_f, (c) the extent of CO_2 disequilibria, (d) sea surface temperature.

Clim. Past Discuss., https://doi.org/10.5194/cp-2018-152
Manuscript under review for journal Clim. Past
Discussion started: 7 November 2018

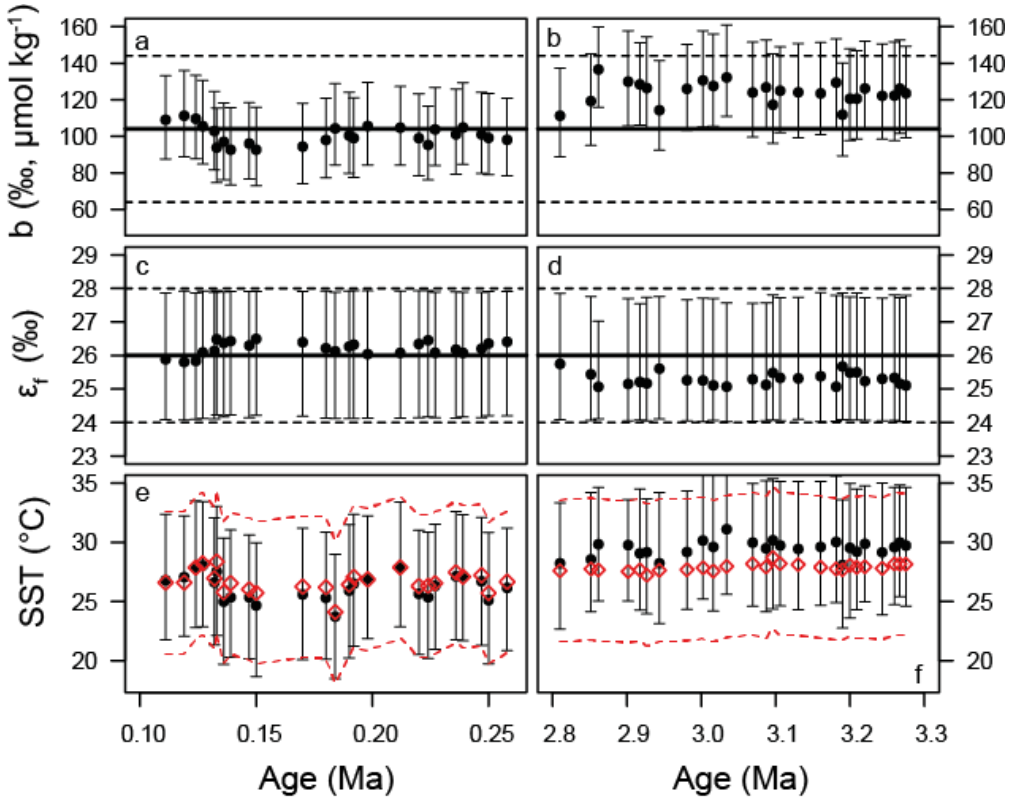

Figure 8. Timeseries of priors and posteriors for the b-term (a, b), ε_f (c,d) and SST (e,f). The Pleistocene is shown on the panels on the left and the Pliocene on the right. In panels a-d the mean of the prior distribution is shown as a thick black line. For the b-term 95% of the input distribution is shown as a dotted line, for ε_f the total range is shown. See Figure 7 for examples of these distributions as probability functions. For SST (e,f) the prior is shown as red diamonds with 95 % of the distribution shown as the dashed lines. In all panels the median of the posterior distributions are shown as circles with error bars encompassing 95 % of the range.

Clim. Past Discuss., https://doi.org/10.5194/cp-2018-152
Manuscript under review for journal Clim. Past
Discussion started: 7 November 2018

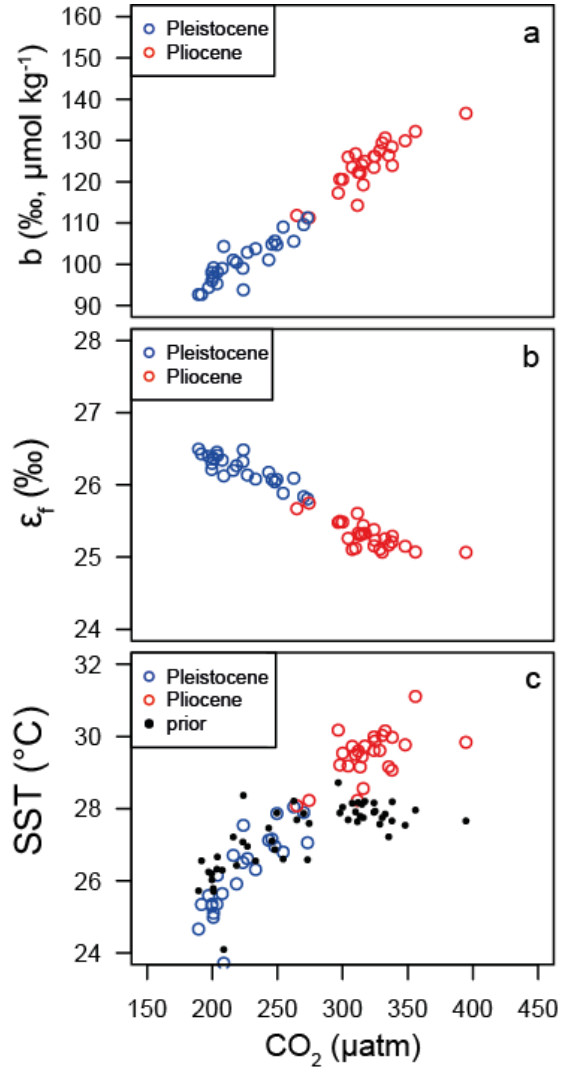

Figure 9. Relationships between CO_2 and (a) b-term, (b) ε_f and (c) SST. In each panel the median of each posterior distribution is shown in red for the Pliocene and blue for the Pleistocene. Note that the CO_2 for each data point is either from the ice core or $CO_{2(\delta 11Bplank)}$ for the Pleistocene and Pliocene, respectively. The linear patterns that emerge here essentially represent the relationships of the Bidigare et al., (1997) **approach given our otherwise invariant ε_p.**